CATHODELESS, HIGH BRIGHTNESS ELECTRON BEAM PRODUCTION BY MULTIPLE LASER BEAMS IN PLASMAS

R.G. Hemker, K.-C. Tzeng, W.B. Mori, C.E. Clayton, UCLA, and T. Katsouleas, USC

Abstract

The use of two crossed laser pulses in a plasma for the cathodeless production of high current low emittance electron beams [1] is examined with fully relativistic 2-1/2D Particle-in-Cell (PIC) simulations. Estimates for the number of injected particles, their energy spread, and their emittance are given as functions of the amplitude and timing of the injection pulse relative to the drive pulse of the LWFA. The physical mechanism of the trapping of particles is examined based on single particle phase space trajectories in the self-consistent PIC simulations.

1 INTRODUCTION

Recently D. Umstadter et al.[1] proposed the use of two orthogonal laser pulses in a plasma to trap and accelerate an ultra-short bunch of electrons. As envisioned the first (or drive) pulse creates a plasma wave which is below its self-trapping or wavebreaking threshold. The transverse ponderomotive force of the second (or injection) pulse gives electrons an extra kick forward in the wake direction, enabling them to be trapped and accelerated in the wake of the drive pulse (fig. 1). Such a cathodeless injector is of interest for a wide variety of applications including as an injector for future linear accelerator technologies with short wavelength accelerating structures. The scheme also naturally overcomes problems of synchronizing the injector with a plasma based accelerator.

In this article, we present results from a detailed two-dimensional (2D) PIC simulation analysis of this concept. We find that our results clearly support the feasibility of such a cathodeless injection scheme, but that the physical mechanism for the trapping is different from the one originally suggested at least for the parameter regime studied in this paper. We will show that the number of particles, emittance , and energy spread can all depend sensitively on the laser parameters and the injection phase. These results place constraints on the allowable shot to shot jitter of the injection laser. Last, based on the new insight into the trapping mechanism, we put forth additional geometries, e.g., co- and counter-propagating pulses, as well as related injection

1 SIMULATION RESULTS

The simulations are conducted with the single node version of the fully relativistic 2-1/2D PIC code Pegasus[2]. This code implements a moving simulation box that can follow the laser pulse for extended periods of time. Pegasus uses the charge conserving algorithm algorithm in ISIS and solves locally for E and B fields. Fig. 1 shows the basic set up of the simulations.

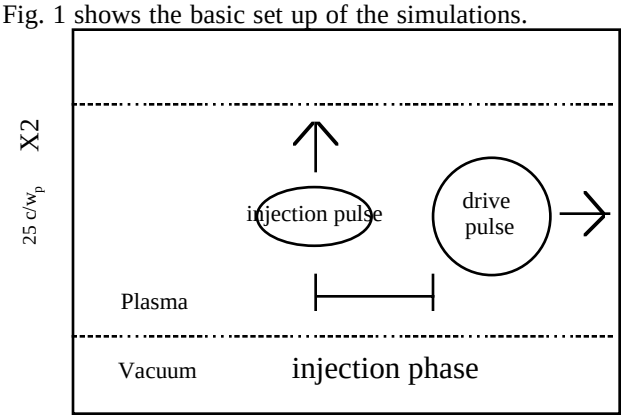

Fig. 1

Fig. 1. Geometry of the cathodeless injector concept. The injection phase of the injection pulse is defined by the distance between the trailing edge of the drive pulse and the center of the injection pulse when it crosses the drive pulse.

In each of the simulations a drive pulse starts to move in the x_1 direction and at a later time an injection pulse is launched from a vacuum region at the side of the box propagating in the x_2 direction as illustrated in fig. 1. The following parameters are valid for most of the simulations evaluated below and should be assumed for all of the results presented if not stated differently. The frequency ratio ω_0/ω_p between the laser frequency and the plasma frequency is 5 for both; thus the simulations have fewer laser cycles than is typical in experiments. Both pulses have their polarization in the plane of the simulation. For the drive pulse the normalized vector potential is $a = eA_y/mc^2 = 1.00$. For the injection pulse the normalized vector potential is $b = eA_x/mc^2 = 2.0$ unless stated otherwise. The transverse profile is given by a gaussian. Both the drive and the injection pulse have a spot size of $3c/\omega_p$. The pulse length, full width from zero to zero, is $2\pi c/\omega_p$ for the drive pulse and $\pi c/\omega_p$ for the injection pulse. We define the injection phase ψ to be the distance between the back of the drive pulse and the center of the injection pulse as it crosses the axis (fig. 1).

The engineering results of the simulations are summarized in fig. 2. In order to convert the simulation results to physical units, we assume a plasma density of $10^{16}cm^{-3}$. Note that the number of electrons as well as the

0-7803-4376-X/98/$10.00 © 1998 IEEE

normalized emittance both scale with $n^{-1/2}$[3]. All quantities including the energy spread are calculated after the final timestep of the calculation. The energy of the trapped particles is around 10 MeV at that time (compared to a theoretical maximum value of about 25MeV for these simulations).

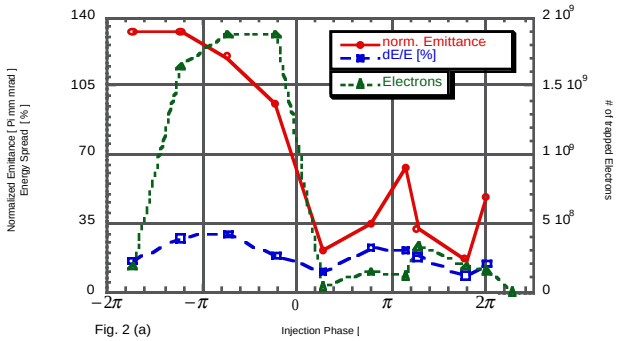

Fig. 2. (a) The number of trapped electrons, the normalized emittance, and the energy spread of the trapped particles as a function of the injection phase. The injection amplitude b is 2.0.

In fig. 2a we plot the number of trapped electrons, the normalized emittance, and the energy spread as a function of the injection phase for a fixed value of the injection amplitude. That value is b = 2.0. Note that negative values for ψ mean that the center of the injection pulse crosses before the end of the drive pulse. The most notable feature of fig. 2a is the great variation of the three beam quantities as a function of ψ and especially the strong difference in the number of particles and their emittance between positive and negative injection phases. The direct overlap of the injection pulse with the drive pulse (i.e. negative injection phase) clearly yields the largest number of trapped particles. The maximum number of trapped electrons corresponds to 1.9 x 10^9 at a plasma density of 10^{16}cm^{-3} (or to 6 x 10^7 at a density of 10^{19}cm^{-3}). The number decreases by an order of magnitude for positive injection phases. The emittance on the other hand is smallest for the positive injection phases, corresponding to the smallest normalized value of 16π mm mrad in a 10^{16} cm^{-3} density plasma (or 0.5π mm mrad at 10^{19} cm^{-3}). It increases by a factor of five for negative injection phases. We believe that the relatively larger emittance and number of particles at negative ψ are both due to stochastic motion of the plasma in the overlapping laser fields. The energy spread of the accelerated bunch does not vary as significantly as the particle number and emittance ; it is between 8% and 22% at a beam energy of 10 MeV and would be expected to scale as $1/\gamma$ if the simulations with larger dephasing energies were done. There is an interesting periodicity to the curves in fig. 2a. The energy spread, and to some extend the number of particles, oscillate with a period of roughly 2π, suggesting that they follow the periodicity of the accelerating plasma wave field. The emittance oscillates with a period of π which follows the periodicity of the magnitude of the focusing field of the accelerating wake.

Although the simulations with b = 2.0 produce similar numbers of particles at $\psi = 1.3\pi$ or 1.8π, as can be seen from fig. 2a, for b =1.8 the number of particles changes from several 10^8 at $\psi = 1.3\pi$ (see fig. 2b) to nearly zero at $\psi = 1.8\pi$ (data not shown in figures). The results of the simulations are therefore sensitive to these parameters and the curve found in fig. 2a for the injection phase dependence at injection amplitudes of 2.0 is not readily applicable to other values of this parameter.

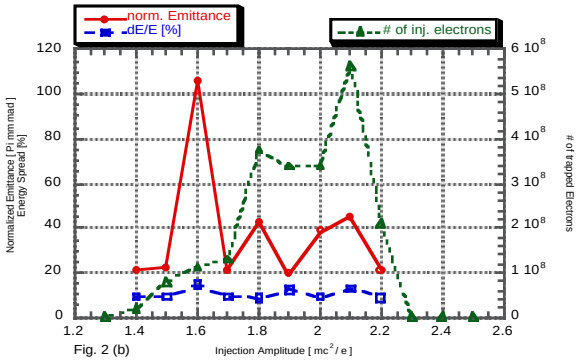

Fig. 2. (b) The number of trapped electrons, the normalized emittance, and the energy spread of the trapped particles as a function of the injection amplitude. The injection phase ψ is 1.3π.

In fig. 2b we plot the same quantities as in fig. 2a but as a function of the injection amplitude for a fixed value of the injection phase ψ. The value of $\psi = 1.3\pi$ is chosen for the simulations of fig. 2b since it seems to be close to an optimal injection phase judging from the data of fig. 2a. As a function of the injection amplitude the normalized emittance and the energy spread do not seem to show any systematic behavior on the scale that is resolved by our simulations. The values of the energy spread vary between 8 % and 15 %, while most of the values for the emittance are between 20 π mm mrad and 50 π mm mrad. In one case the emittance goes up to 106 π mm mrad. This means that the beam quality is quite sensitive to variations in the injection amplitude. The number of trapped electrons on the other hand shows a systematic behavior. As should be expected the number of trapped particles first rises with increasing injection amplitude and then falls off. We explain this decrease with the increase in transverse momentum (p_z) that is transferred to the particles by the injection pulse. At a certain value this transverse momentum becomes large enough to prevent the trapping of the particles.

The above results indicate that the properties of the electron bunches obtained in the simulation is promising. We give here the values for the simulation at $\psi = 1.8\pi$ with an injection amplitude of a = 2.0 interpreted at a density of n = 10^{16}cm^{-3}. The average current of a bunch is 170 A. The normalized brightness is 6.8 x 10^{10} A/m^2. The beam is not space charge dominated [4]. It is an approximately matched beam and its emittance is about 10% of the acceptance of the plasma wave[3]. The beam density is 3x10^{14}cm^{-3}, 3% of plasma density. Note that the beam brightness and density increase linearly with the plasma density.

To gain a deeper understanding of the process we follow the momentum of a single, typical, trapped particle as function of time in the 2D simulation. We consider a particle for the case of $\psi = 1.3\pi$ and b = 1.8. The data are shown in fig. 3. The initial momentum is zero since the simulation uses cold plasma.

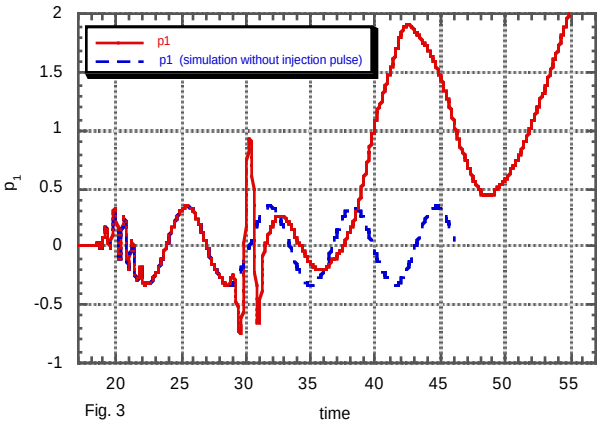

Fig. 3. p_1 of a test particle as a function of time. The two curves are the results from simulations with (solid) and without (dashed) an injection pulse. $\psi = 1.3\pi$ and b = 1.8 for the simulation with an injection pulse.

The solid curve in fig. 3 shows the longitudinal momentum of the particle; the dotted curve shows p_1 for the same particle in a simulation were the injection pulse is not launched but that is otherwise identical. As expected, this particle simply oscillates in the wake of the drive pulse. In the full simulation we can see that the injection pulse has completely passed by the test particle at about the time t=31.7. Although the injection pulse has an impact on the particle, the really large changes occur later at a time when the injection pulse has already left the area of the test particle. This means that the particle gets the actual momentum needed for getting trapped not from any effect directly related to the laser pulses (since those have already left the area of the particle), but by effects related to the interaction of the two plasma wake fields created by these pulses. Note that the trapped particle goes through one full oscillation (accelerating, decelerating, and accelerating again) before it is trapped. This feature that the particles get accelerated above the trapping threshold in a multi-step process (acceleration-deceleration-acceleration) caused by the interaction of the wake fields is not unique to this particular simulation. Other simulations with different values for ψ and b show the same process.

1 CONCLUSIONS

In this paper, we have found that the beam brightness and quality found in our simulations compares reasonably with that of electron bunches produced by other technologies. The mechanism for the trapping of particles is not the transverse ponderomotive force of the injection pulse, rather it comes from the interaction of the particles with the two plasma wakes. It should be noted however that this does not rule out the possibility that a different choice of parameters for the injection pulse might result in trapping due to a direct kick by the transverse ponderomotive force. The results of our research open up a number of possibilities for future investigations.

Two important goals of future research would be to find an analytical model of the process that is able to predict the results seen in the simulations and to use 3D PIC simulations. This will facilitate optimizing parameters and determining what are the fundamental limits on beams produced by this scheme. Secondly additional geometries need to be investigated , such as co- and counter-propagating drive and injection lasers. The crucial idea here is that the Rayleigh length of the injection pulse is much shorter than the Rayleigh length of the drive pulse. This means that the injection pulse will interact significantly with the plasma only for a short distance. Our preliminary results show that the combined plasma wakes have an amplitude that is temporarily large enough to cause local wavebreaking. The fact that the plasma wave is responsible for the trapping of particles in our simulations suggests also to investigate other ways to excite this plasma wave that causes this trapping. If a method could be used that builds up the plasma wave gradually over time like a PBWA[5], then less powerful lasers would be required.

This work was supported by DOE Grant No. DE-FG03-92ER40727 and LLNL.

REFERENCES

[1] 'D. Umstadter, J.K. Kim, and E. Dodd, Phys. Rev. Lett. **76**, 2073 (1996).
[2] K.-C. Tzeng, W.B. Mori, Phys. Rev Lett. **76**, 3332 (1996).
[3] R.G. Hemker, K.-C. Tzeng, W.B. Mori, C.E. Clayton, T. Katsouleas , submitted to Phys. Rev. E.
[4] J.D. Lawson, The Physics of Charged Particle Beams, 2nd Ed. (Oxford Univ. Press, New York, 1988).
[5] IEEE Trans. Plasma Sci., vol. **24**, no. 2.